

NEARBY GALAXIES IN MORE DISTANT CONTEXTS

MICHAEL ESKEW AND DENNIS ZARITSKY

Steward Observatory, University of Arizona, 933 North Cherry Avenue, Tucson, AZ 85721, USA

Submitted to the Astronomical Journal

ABSTRACT

We use published reconstructions of the star formation history (SFH) of the Large Magellanic Cloud (LMC), Small Magellanic Cloud, and NGC 300 from the analysis of resolved stellar populations to investigate where such galaxies might land on well-known extragalactic diagnostic plots over the galaxies' lifetime (assuming that nothing other than their stellar populations change). For example, we find that the evolution of these galaxies implies a complex evolution in the Tully-Fisher relation with lookback time and that the observed scatter is consistent with excursions these galaxies take as their stellar populations evolve. We find that the growth of stellar mass is weighted to early times, despite the strongly star-forming current nature of the three systems. Lastly, we find that these galaxies can take circuitous paths across the color-magnitude diagram. For example, it is possible, within the constraints provided by the current determination of its SFH, that the LMC reached the red sequence at intermediate age prior to ending back up on the blue cloud at the current time. Unfortunately, this behavior happens at sufficiently early times that our resolved SFH is crude and insufficiently constraining to convincingly demonstrate that this was the actual evolutionary path. The limited sample size precludes any general conclusions, but we present these as examples how we can bridge the study of resolved populations and the more distant universe.

Subject headings: galaxies: evolution

1. INTRODUCTION

The universe has made it both easier and more difficult to study galaxy evolution than it could have. We are grateful for the finite speed of light, which enables us to observe distant galaxies when they are young (in the cosmological sense). On the other hand, we are frustrated (at least in this sense) with the grave mismatch in galactic and human timescales that precludes us from observing any individual galaxy as it evolves. As such, we have relied on observing changes in galaxy ensembles (cf. Butcher & Oemler 1984) across cosmic time and testing simple evolutionary models against such observations (cf. Tinsley 1972). These theoretical exercises are statistical consistency checks and do not directly verify the unique ability of any particular model to represent galaxy evolution.

How convoluted could the actual evolutionary history of each individual galaxy be? To study the evolution of a single galaxy requires us at a minimum to understand the rate at which it formed stars over its history. Of course, there are other aspects of a galaxy's evolution, including the accretion of both dark matter and baryons, that are harder to constrain. Even so, the relatively straightforward study of the star formation history (SFH) of galaxies has been fairly limited to date. Due to technical limitations, such work has focused almost exclusively on Local Group galaxies (Tolstoy, Hill, & Tosi 2009), although the superior angular resolution of space-based telescopes has allowed us to begin a systematic extension to galaxies outside the Local Group (for example, see Dalcanton et al. 2009). This extension is critical because the galaxies one can study at larger distances are intrinsically brighter (by many magnitudes) than the typical Local Group galaxy, and therefore more repre-

sentative of unresolved galaxies studied at even larger distances. Bridging the study of a relatively small number of resolved galaxies and that of statistically large samples at higher redshift has proved difficult. Here we examine how a small set of local galaxies behave as their stellar populations evolve on some well-known diagnostic plots that are often used to characterize unresolved galaxies. The aim of this exercise is to begin formulating intuition about the nature of the scatter in these relations and any systematic behavior with time. We focus on the two most luminous Local Group galaxies for which global SFHs have been measured (the Large Magellanic Cloud (LMC) and the Small Magellanic Cloud (SMC); Harris & Zaritsky 2004, 2009) and one additional relatively massive, nearby galaxy for which a nearly global history has been published (NGC 300; Gogarten et al. 2010).

2. RECONSTRUCTED GALAXY EVOLUTION

We begin with the published star formation rates (SFRs) as a function of time for the three galaxies of interest. These are then converted into luminosities, colors, and stellar masses over time using the population synthesis code, PÉGASE (Fioc & Rocca-Volmerange 1997, although we use their updated Version 2 from 2001). PÉGASE produces a historical record of observable galactic characteristics using the input galactic SFH and specified input parameters, such as the stellar initial mass function. Unless otherwise stated, we adopt the default parameter values. Given the limited number of galaxies in our sample, this is not a parameter study and we opt for simplicity. There are, of course, various limitations that will eventually restrict what one can do with this approach. The most important of these is that the temporal resolution of the SFHs is itself a function of time and generally degrades, resulting in temporal resolution

that is roughly constant with $\log(\text{age})$.

For most general studies of galaxy evolution that use PÉGASE, the adopted input SFH is specified using a simple analytical model such as an exponentially declining SFR (the τ models). Fortunately, for generality, the algorithm was constructed to allow for non-parametric, user-defined histories. We use the source SFHs as published for the LMC (Harris & Zaritsky 2009), SMC (Harris & Zaritsky 2004), and NGC 300 (Gogarten et al. 2010). For the LMC and SMC we combine the SFHs from all spatial bins to produce a single, global SFH. For NGC 300 we also combine SFHs from the spatial bins, but because the coverage is not complete we normalize each by the inverse of the fractional area observed at that radius to obtain an estimated global SFH. This ratio is calculated using the size of the observed field and the area of the full aperture at the given radius. We ignore the metallicity information provided by these sources (thereby allowing PÉGASE to calculate an internally consistent chemical evolutionary history). The assumption of internally self-consistent evolution has been shown to fail in detail for the SMC by Zaritsky & Harris (2004), which they interpret as the need for gaseous infall, but we ignore that additional level of complication here.

In detail, some slight adjustments to the published SFHs are needed in the interest of uniformity. We modify each SFH to cover 14 Gyr by extending or contracting the initial time bin in the published versions when necessary, proportionately decreasing or increasing the SFR so that the total number of stars produced remains unchanged. There remains a slight tension between ages determined from stellar models and those from the currently standard Lambda cosmology ($\Omega_m = 0.27$, $\Lambda = 0.73$, $H_0 = 70 \text{ km s}^{-1} \text{ Mpc}^{-1}$) in that the oldest isochrones used tend to be older than the age of the universe. However, a modest change in the value of H_0 to 67, for example, allows ages up to 14.5 Gyr, which we use as our upper limit. Any stars formed from isochrones with stated ages older than 14.5 Gyr are incorporated into this oldest bin. Our temporal resolution at these ages is extremely coarse, so we are insensitive to such distinctions although they remain a numerical oddity. Alternatively, we also ran models where every age bin was narrowed by a constant fraction to provide consistency between the total age and cosmological constraints. These models produced no significant differences, with one exception that we discuss further in Section 3.2. In all other cases, we present the results only from the first approach.

To produce a relatively accurate self-consistent model, the algorithm must account properly for both the stars formed and the gas consumed (and recycled). The model naturally begins with all of its mass in the gas phase, but the gas mass relative to the final stellar mass is a free parameter. A given SFH could result either in a gas-rich or gas-poor galaxy depending on how much gas the system begins with. To remove this degeneracy, we require that the model produce the current observed gaseous to stellar mass ratio for each galaxy. The PÉGASE models work on the basis of evolving 1 M_\odot of gas. We scale the SFH so that the final ratio of mass in gas to stars matches observations. We adopt measurements of the current gas masses from Staveley-Smith et al. (2003)

and Mizuno et al. (1999) for the LMC, Tumlinson et al. (2002) for the SMC, and de Vaucouleurs & Page (1961) for NGC 300. Lastly, we scale the mass of the entire system so that the final stellar mass matches the integral of the published SFHs.

Once these quantities are determined, PÉGASE straightforwardly calculates the colors, luminosities, and stellar masses at each age. These output values enable us to place our galaxies on the diagnostic plots.

3. DISCUSSION

With the stellar population evolutionary histories of these galaxies in hand, we now investigate how these galaxies move across three different, but common, diagnostic plots. First, we explore their behavior on the Tully-Fisher relationship (Tully & Fisher 1977). This scaling law is commonly used to explore disk galaxy evolution, with the expectation that systemic evolution of the sizes or luminosities of the galaxies might lead to zero point and/or slope changes in the relationship (cf. Weiner et al. 2006, and references therein). Second, we explore their behavior on the stellar-mass density versus redshift (or age) plot. Ensembles of galaxies across many redshifts are used to construct the plot that shows when the universe creates its stars (cf. Rudnick et al. 2006, and references therein). Of course, such measurements represent ensemble averages, so it is worthwhile to compare with how individual galaxies build their stellar populations. This exercise is being done for a large sample of dwarf galaxies (Weisz et al. 2010) and our sample overlaps that one slightly and extends the coverage toward more massive systems. In particular, there are claims of generic galaxy behavior in which low-mass galaxies form more of their stars later (more recently) than more massive galaxies (“downsizing”; Cowie et al. 1996). However, the term “downsizing” has confusingly been used in many different ways (for an explanation of various forms of downsizing see Fontanot et al. 2009). We will test whether such trends are evident for at least these three galaxies. Lastly, we explore the galaxies’ behavior on the color-magnitude diagram of galaxies. Here the questions relate primarily to how or whether galaxies migrate between the various identified populations (eg. red sequence, green valley, blue cloud). The general expectation is that galaxies migrate (eventually) from the blue cloud through the green valley onto the red sequence, although all three of our galaxies are currently star forming.

3.1. The Tully-Fisher Relation

Using the results from the PÉGASE modeling, we present the evolution of the three galaxies on the TFR and compare them with the current positions of 162 spiral galaxies (Pizagno et al. 2007) and of 87 isolated, low-mass galaxies (Blanton et al. 2005). Rotation values for the LMC (Alves & Nelson 2000), SMC (Stanimirovic et al. 2004), and NGC 300 (Puche et al. 1990) are taken to be constant in time.

The current positions of the three galaxies fall well within the scatter extrapolated from the distribution of spiral galaxies (Figure 1), suggesting that there is no fundamental problem with the calculated current-day magnitudes from our modeling. The SMC lies at the lower

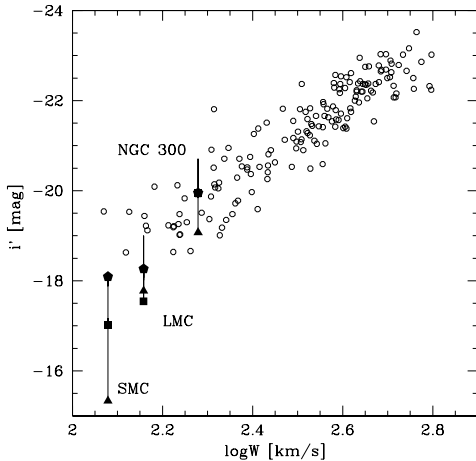


FIG. 1.— Evolution of galaxies on the Tully-Fisher relation. Open symbols represent the 162 SDSS galaxies studied in the compilation by Pizagno et al. (2007). The solid symbols represent the SMC, LMC, and NGC 300 with the solid line tracing their evolution and the symbols representing different ages (triangle: 0.5 Gyr; square: 8 Gyr; pentagon: current-day).

end of the range in rotation speeds for the Sloan Digital Sky Survey (SDSS) galaxies, highlighting how poorly most Local Group galaxies match those studied beyond the Local Group. Even our most massive galaxy, NGC 300, does not reach the median rotation value of this local sample. The problem becomes increasingly acute when studying cosmologically interesting samples.

The LMC and NGC 300, the two galaxies that are somewhat more representative of the SDSS sample, spend their entire lifetime within the scatter of the current-day positions of the SDSS galaxies. Assuming that the fluctuations in star formation experienced by these galaxies is not synchronized, this finding suggests that much of the observed TFR scatter could be due to variations in stellar populations. In contrast, investigators have searched for correlations between TFR residuals and color (Kannappan et al. 2002; Pizagno et al. 2007) and found little or none. It is unclear the extent to which that type of investigation is complicated by internal extinction and geometry, and to which our results may not be representative of more massive (typical) TFR galaxies.

Although the SMC shows a systematic brightening over time, as one might expect as a galaxy progressively forms more stars, both the LMC and NGC 300 are not currently at their brightest luminosity. These two galaxies move up and down within the observed TFR scatter over their lifetime, suggesting that there may not be a simple coherent evolution of the TFR with redshift. On the other hand, even if the evolution is not monotonic, the TFR may still be a powerful diagnostic to the degree that evolution is synchronized for galaxies of a given mass. For example, in a scenario where the massive galaxies form most of their stars first and the intermediate galaxies, such as NGC 300 and the LMC, are more vigorously forming stars now, one might expect the TFR to be steeper in the distant past relative to the current

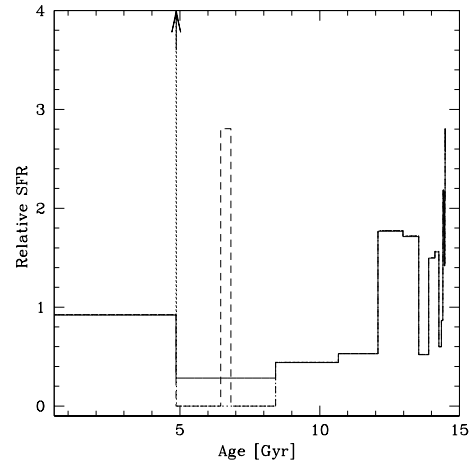


FIG. 2.— Star formation history of the LMC. The solid line represents the baseline model of the star formation history of the LMC (see Harris & Zaritsky (2009) for details). Current-day is at the right of the figure. The dotted line represents Burst Model 1 (BM1, see the text for details) with a burst at ~ 5 Gyr. This burst reaches ~ 66 on the y-axis. The dashed line represents Burst Model 2 (BM2) with a longer period of more modestly elevated star formation at ~ 6.5 Gyr.

TFR. Interestingly in this regard, the luminosities of the LMC and NGC 300 do behave similarly with time.

One important hidden aspect of the SFHs we use is that we only constrain the number of stars formed over a fairly large amount of time, particularly for ages > 5 Gyr. Within a bin, we have no constraint on the fluctuations in the SFR. To study possible effects of unresolved bursts, we create two models for the LMC that probe a range of possibilities. In our Burst Model 1 (BM1), we place all of the star formation in our second oldest bin, which happens to be the one with the longest age span, into as small a burst as we ever resolve (~ 20 Myr). This is evidently a completely unrealistic, extreme scenario, but it illustrates the maximum impact that an unresolved, ancient burst would have on our results. In our Burst Model 2 (BM2) we create a modestly elevated SFR, corresponding in magnitude to what is typical at more recent times where we have better resolution. We define the length of that “burst” so that it produces the same total number of stars over the corresponding bin as in our baseline SFH. This scenario represents the smallest unresolved variation that we should expect. These two burst models are graphically illustrated in Figure 2.

The results of these burst models are that the TFR evolution is likely to be qualitatively unaffected by unresolved bursts. BM2 produces a TFR history (Figure 3) that is effectively indistinguishable from that shown in Figure 1. Even for BM1, the LMC’s luminosity, while noticeably larger than in the baseline model, still places the galaxy within the TFR scatter. If the TFR scatter has several contributing components, then it will be difficult to use residuals from the TFR to infer variations in SFR of a scale seen in the LMC and NGC 300. The apparent “scatter” due to SFH variations will be present regardless of what additional complications, such as mass

accretion, are occurring.

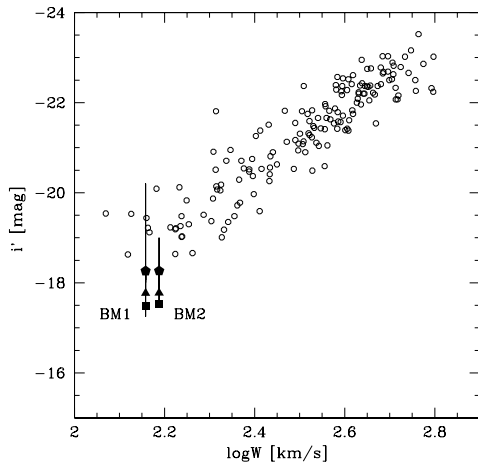


FIG. 3.— Effect of star formation bursts on the Tully-Fisher relation. Symbols represent the same as in Figure 1 although the LMC evolution is now shown for the Burst Model 1 (BM1; left) and Burst Model 2 (BM2; right). BM1 represents an extreme scenario that is unrealistic but is meant to explore the maximum effect of unresolved star formation episodes. BM2 is a more realistic model meant to match the variation in star formation rates seen currently. The two models are displaced horizontally for clarity, with BM1 being at the correct location for the LMC.

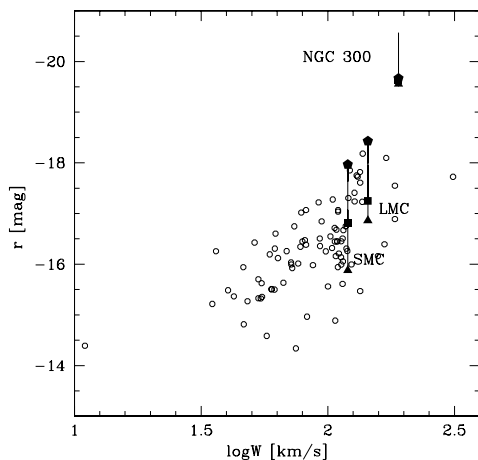


FIG. 4.— Evolution of galaxies on the Tully-Fisher relation. Open symbols represent the 87 galaxies studied in the compilation by Blanton et al. (2005), corrected to match the gas fraction of the Clouds (see the text for details). The solid symbols represent the SMC, LMC, and NGC 300 with the solid line tracing their evolution and the symbols representing different ages (triangle: 0.5 Gyr; square: 8 Gyr; pentagon: current-day).

One shortcoming of the previous comparison is the limited overlap between the Pizagno et al. (2007) galaxies and our sample of three, particularly with the two Magellanic Clouds. In an effort to address this issue, we

utilize the data from Blanton et al. (2005), who investigated the TFR for low-luminosity, isolated galaxies. By its nature, this sample consists of fairly gas-rich galaxies that often have the majority of their baryons in the gas phase rather than the stellar phase. This characteristic complicates the comparison to our sample because the Clouds are relatively stellar dominated (both have roughly 75% of their baryons in the stellar phase). To mitigate this difference, we “convert” a fraction of the gas in the Blanton et al. (2005) galaxies into stars, using the M/L value adopted by Blanton et al. (2005), and by doing so calculate the luminosity of these galaxies if they too had 75% of their baryons in the stellar phase (this is analogous to placing galaxies on a baryonic TF; see McGaugh et al. (2000)). The comparison of their TFR to our galaxies is shown in Figure 4. This comparison leads to the same conclusions as those described previously for the comparison to the Pizagno et al. (2007) galaxies, although here our galaxies are at the upper end of the $\log(W)$ range.

3.2. Stellar Mass Evolution

The opening of the higher redshift ($z > 0.5$) universe of galaxies to observations has provided clear evidence for the modulation in the overall rate of star formation with lookback time (Lilly et al. 1996; Madau et al. 1998). Common diagnostic plots of the stellar populations in galaxies now include both the differential (the SFR or “Madau” plot) and the integral form (the stellar mass density). In Figure 5, we plot the fraction of the stellar mass formed as a function of time for each galaxy, including the baseline LMC model and the two burst models, and compare to several sets of published data for the stellar mass density as measured from ensembles of high-redshift galaxies. This comparison, specifically for the LMC, is the only case where our treatment for addressing the internal inconsistency between our oldest stellar populations and the age of the universe results in significantly different results. Using the approach where we simply truncate the oldest bin results in the LMC being discrepant with the high-redshift sample at a level comparable to that for NGC 300, whereas the curves shown in Figure 5 correspond to the approach where we proportionally trim the length of each time bin. The alternative approaches do not result in significant differences for NGC 300 and the SMC.

It is evident that NGC 300 forms fractionally more stars at early times than the bulk of the cosmologically measured galaxies. The SMC and LMC either follow the high-redshift trend or lie only slightly below it. The sense of these results runs counter to a simple interpretation of the “downsizing” concept because these relatively low-mass galaxies did not form their stars at more recent times than the bulk of higher mass galaxies observed at high redshifts. However, our sample of three does indeed follow the trend in that the stellar fraction is always higher in the more massive galaxy.

We conclude that we see few or no signs from this small sample that low-mass galaxies have necessarily formed a larger fraction of their stellar populations more recently than did higher mass galaxies, unless one refers to SMC-like and lower mass galaxies as those participating in the phenomenon. Of course, the LMC and SMC are perhaps unusual in that they are close to the Milky Way, although

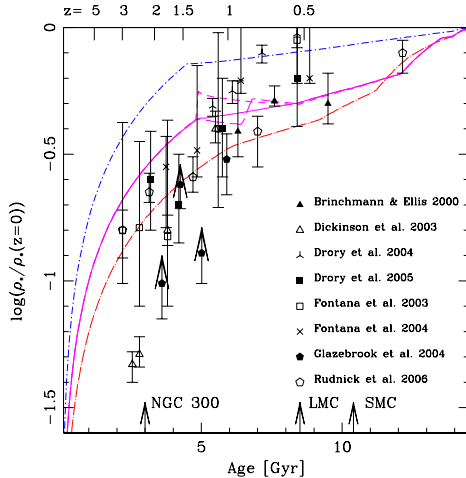


FIG. 5.— Growth of stellar mass. Symbols represent data from ensembles of high-redshift galaxies taken from the cited studies and the format of the plot follows Rudnick et al. (2006). The lines represent the results for our three galaxies: the LMC, NGC 300, and SMC going from highest to lowest at $z = 5$. Additionally, the line for each galaxy is identified by color in the online version of the plot: LMC tracks are in magenta, SMC track in red, and NGC 300 track in blue. The two dashed lines tracing the baseline LMC result represent two different alternate SFHs for the LMC (BM1 and BM2, see the text for details). The labeled arrows at the bottom mark the time by which 50% of the current stellar mass has formed.

some suggest that the LMC/SMC are on their first approach toward the Milky Way (Besla et al. 2007). There are ways around the apparent paradox. For example, if the ensemble work is missing a significant ancient stellar population in galaxies, then it has an incorrect normalization relative to our galaxies. Missing such a population would not necessarily affect the relative comparison of massive and less massive galaxies within the ensembles, but would distort the comparison to our galaxies.

3.3. The Color-Magnitude Diagram

The color-magnitude diagram exemplifies the interesting bimodality of galaxies. The red sequence contains the non-star-forming, generally pressure-supported galaxies, while the blue cloud contains the star-forming, generally rotationally supported galaxies. Although some exceptions exist (Chen et al. 2010), the general evolution model that is envisioned (cf. Bell et al. 2004) is that at some point in their history, perhaps as a result of an interaction, blue cloud galaxies move toward the red sequence passing through the intermediate region termed the green valley. This is a fairly orderly picture of galaxy evolution and is supported by the observed growth in the number of galaxies on the red sequence, particularly at fainter magnitude (De Lucia et al. 2007). However, individual galaxies may not be so well behaved.

In Figure 6, we show the color and magnitude evolution of the LMC, the SMC, and NGC 300 in comparison to the current-day distribution of over 4×10^5 SDSS galaxies (Blanton et al. 2005). The evolutionary tracks show that after the initial phase, which is a blue hook and not well constrained by the available SFHs, the galaxies all progress onto the blue cloud. Their evolutionary paths

take them through the large range of colors seen in the blue cloud, but not beyond it. As such, we might conclude that the picture of galaxies remaining in the blue cloud prior to any possible, eventual migration onto the red sequence is correct. However, these models represent the minimum excursion set because we average the SFR within a given time bin.

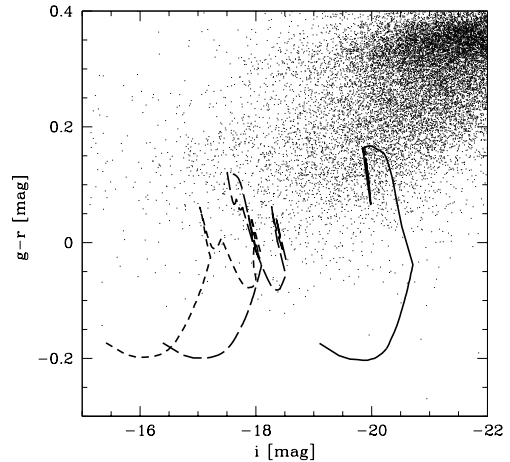


FIG. 6.— Evolution of galaxies on the color-magnitude diagram. We plot the evolutionary paths of the SMC, LMC, and NGC 300 from left to right, respectively, on the distribution of local galaxies from SDSS. All galaxies begin at the lower left extreme of their track and move as time progresses toward the blue cloud. The evolutionary paths are mostly constrained to lie in the “blue cloud” of galaxies and all galaxies are currently in the blue cloud.

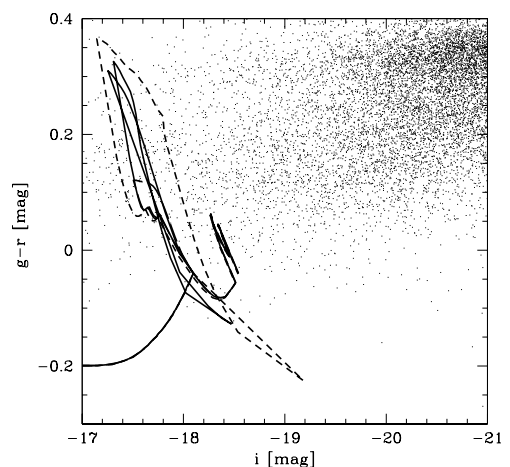


FIG. 7.— Different possible evolutionary paths for the LMC on the galaxy color-magnitude diagram. We plot the evolutionary paths of the LMC in the baseline model (long-dashed line), BM1 (short-dashed line), and BM2 (solid line). Both alternate models have the LMC reaching colors as red as the red sequence before returning to the blue cloud once star formation starts again.

We show a range of possible behavior for the LMC in Figure 7. We plot our baseline model, BM1, and BM2. BM1 with its rather extreme burst shows a path by which the LMC would reach the red sequence prematurely. This result may at first seem contradictory in that adding a burst has enabled the LMC to reach the red sequence. This behavior occurs because we have a constraint on the total SFR within the bin, and therefore, placing a burst at one time implies a deficit in star formation at all other times. Of course, BM1 is an unrealistic, extreme scenario, but BM2, which is consistent in amplitude with the bursts seen at recent times, also takes the LMC to the red sequence.

We conclude that our SFHs do not exclude eras of quiescence that would allow a galaxy like the LMC to evolve from the blue cloud onto the red sequence, only to have it later evolve back into the blue cloud once star formation sufficiently re-engages. This exercise highlights both the potential and limitations of the approach we are taking. At face value, the current SFHs support a model in which these galaxies have always been among the blue cloud galaxies. However, the current data are insufficient to answer the question of whether these galaxies wandered onto the red sequence only to return to the blue cloud. Deeper, higher resolution data from which higher temporal resolution SFHs could be constructed would help address this question. Nevertheless, it is evident that galaxies will move significantly, and stochastically, as they evolve within this diagram.

4. SUMMARY

We illustrate how SFHs, reconstructed from the resolved stellar populations of nearby galaxies, can be used to build intuition regarding the behavior of individual galaxies in diagnostic plots used more commonly to study the behavior of galaxy ensembles at greater distances. Specifically, we investigate the behavior of the SMC, LMC, and NGC 300 in the TFR, the stellar mass versus cosmic time plot, and the color-magnitude diagram of galaxies.

The three galaxies we investigate all currently fall within the observed local TFR. However, their evolution

drives them across the full range of the scatter, suggesting that variation in the SFH contributes significantly to the observed scatter. We also find that the evolution we measure in the stellar populations does not result in a monotonic drift relative to the relation, thereby suggesting that an ensemble of galaxies may not show evident zero point or slope changes over redshift, or that those changes may be weaker than otherwise expected.

The three galaxies we investigate all show stronger early growth in their stellar mass than the average for field galaxies. This result is also found for a larger sample of lower mass, local dwarf galaxies by Weisz et al. (2010). This result brings to question a simple model of “downsizing” where low-mass galaxies form a larger fraction of their stars after the more massive galaxies. While the current SFRs of the three galaxies here place them all among blue, star-forming galaxies, the data show that star formation in these systems was not wholly delayed until relatively recent times.

The three galaxies we investigate all trace paths that populate the blue cloud of the color-magnitude diagram. However, at least one plausible SFH, in that it is allowed within the range of uncertainties in the current measurement of the LMC SFH, has the LMC reaching the red sequence before returning to its current location among the blue cloud galaxies. As such, we cannot exclude the possibility that galaxies wander across populations in the diagram rather than systematically proceeding from blue cloud to red sequence.

The current study is limited by sample size, temporal resolution, and the lack of higher mass galaxies that are more representative of the class of galaxy observed at higher redshifts. Nevertheless, it exemplifies some of what might be possible when resolved SFHs are used to examine the behavior of individual galaxies on common diagnostic plots.

We thank S. Gogarten for communicating her star formation rate measurements for NGC 300 electronically and acknowledge financial support from NASA LTSA award NNG05GE82G and NSF grants AST-0307482 and AST-0907771.

REFERENCES

- Alves, D., & Nelson, C. 2000, *ApJ*, 542, 789
 Bell, E. F., et al. 2004, *ApJ*, 608, 752
 Besla, G., Kallivayalil, N., Hernquist, L., Robertson, B., Cox, T.J., van der Marel, R.P., & Alcock, C. 2007, *ApJ*, 668, 949
 Blanton, M., et al. 2005, *AJ*, 129, 2562
 Brinchmann, J., & Ellis, R. 2000, *ApJ*, 536, L77
 Butcher, H., & Oemler, A., 1984, *ApJ*, 285, 426
 Chen, Y., Lowenthal, J.D., & Yun, M.S. 2010, *ApJ*, 712, 1385
 Cowie, L.L. Songaila, A., Hu, E.M., & Cohen, J.G. 1996, *AJ*, 112, 839
 Dalcanton, J.J., et al. 2009, *ApJS*, 183, 67
 De Lucia, G., et al. 2007, *MNRAS*, 374, 809
 de Vaucouleurs, G., & Page, J. 1961, *ApJ*, 136, 107
 Dickinson, M., Papovich, C., Ferguson, H.C., & Budavri, T. 2003, *ApJ*, 587, 25 (D03)
 Drory, N., Bender, R., Feulner, G., Hopp, U., Maraston, C., Snigula, J., & Hill, G.J. 2004, *ApJ*, 608, 742
 Drory, N., Salvato, M., Gabasch, A., Bender, R., Hopp, U., Feulner, G., & Pannella, M. 2005, *ApJ*, 619, L131
 Fioc, M., & Rocca-Volmerange, B. 1997, *A&A*, 326, 950
 Fontana, A., et al. 2003, *ApJ*, 594, L9 (F03)
 Fontana, A., et al. 2004, *A&A*, 424, 23
 Fontanot, F., De Lucia, G., Monaco, P., Somerville, R.S., & Santini, P. 2009, *MNRAS*, 397, 1776
 Glazebrook, K., et al. 2004, *Nature*, 430, 181
 Gogarten, S., et al. 2010, *ApJ*, 712, 858
 Harris, J., & Zaritsky, D. 2004, *AJ*, 127, 1531
 Harris, J., & Zaritsky, D. 2009, *AJ*, 138, 1243
 Kannappan, S.J., Fabricant, D. G., & Franx, M. 2002, *AJ*, 123, 2358
 Lilly, S.J., Tresse, L., Hammer, F., Crampton, D., & Le Fevre, O. 1995, *ApJ*, 455, 108
 Madau, P., Pozzetti, L., & Dickinson, M. 1998, *ApJ*, 498, 106
 McGaugh, S.S., Schombert, J.M., Bothun, G.D., & de Blok, W.J.G. 2000, *ApJ*, 533, 99
 Mizuno, N., et al. 1999, in *IAU Symp.*, 190
 Pizagno, J., et al. 2007, *AJ*, 134, 945
 Puche, D., Carignan, C., & Bosma, A. 1990, *AJ*, 100, 1468
 Rudnick, G., et al. 2006, *ApJ*, 650, 624
 Stanimirovic, S., Staveley-Smith, L., & Jones, P.A. 2004, *ApJ*, 604, 176
 Staveley-Smith, L., Kim, S., Calabretta, M.R., Haynes, R.F., & Kesteven, M.J. 2003, *MNRAS*, 339, 87
 Tinsley, B.M. 1972, *ApJ*, 178, 319

Tolstoy, E., Hill, V., & Tosi, M. 2009, ARA&A, 47, 371
Tully, R.B., & Fisher, J.R. 1977, A&A, 54, 661
Tumlinson, J., et al. 2002, ApJ, 566, 857

Weiner, B. J., et al. 2006, ApJ, 653, 1049
Weisz, D., et al. 2010, arXiv:1101.1093
Zaritsky, D. & Harris, J. 2004, ApJ, 604, 167